



# The physical basis of mollusk shell chiral coiling

Régis Chirat<sup>a,1</sup>, Alain Goriely<sup>b</sup>, and Derek E. Moulton<sup>b</sup>

<sup>a</sup>Univ Lyon 1, ENSL, UJM, CNRS, LGL-TPE (Laboratoire de Géologie de Lyon: Terre, Planète, Environnement), 69622 Villeurbanne, France; and <sup>b</sup>Mathematical Institute, University of Oxford, Oxford OX2 6GG, United Kingdom

Edited by Neil H. Landman, American Museum of Natural History, New York, NY, and accepted by the Editorial Board September 30, 2021 (received for review May 18, 2021)

**Snails are model organisms for studying the genetic, molecular, and developmental bases of left–right asymmetry in Bilateria. However, the development of their typical helicospiral shell, present for the last 540 million years in environments as different as the abyss or our gardens, remains poorly understood. Conversely, ammonites typically have a bilaterally symmetric, planispirally coiled shell, with only 1% of 3,000 genera displaying either a helicospiral or a meandering asymmetric shell. A comparative analysis suggests that the development of chiral shells in these mollusks is different and that, unlike snails, ammonites with asymmetric shells probably had a bilaterally symmetric body diagnostic of cephalopods. We propose a mathematical model for the growth of shells, taking into account the physical interaction during development between the soft mollusk body and its hard shell. Our model shows that a growth mismatch between the secreted shell tube and a bilaterally symmetric body in ammonites can generate mechanical forces that are balanced by a twist of the body, breaking shell symmetry. In gastropods, where a twist is intrinsic to the body, the same model predicts that helicospiral shells are the most likely shell forms. Our model explains a large diversity of forms and shows that, although molluscan shells are incrementally secreted at their opening, the path followed by the shell edge and the resulting form are partly governed by the mechanics of the body inside the shell, a perspective that explains many aspects of their development and evolution.**

ammonites,\* a group of extinct mollusk cephalopods with an external chambered shell that populated the seas for 340 million years and became extinct 66 million years ago. Like the extant chambered *Nautilus*, about 99% of 3,000 ammonite genera have nonchiral, bilaterally symmetric shells, most often a planispiral or, more rarely, a straight shell or a combination of both forms, despite the fact that *Nautilus* and gastropods share the same basic structure of the shell-secreting system (6, 7) and that both empirical and theoretical evidences suggest that it was shared by ammonites as well (8, 9). That is, ammonites were likely secreting their shells in the same way as gastropods and yet producing, in the vast majority of cases, symmetric shells. The remaining 1% of ammonites are represented by some 40 genera mostly belonging to seven Cretaceous families displaying, at least during a part of their development, an asymmetric, often helicospiral shell (10). Two asymmetric genera are also known in the upper Triassic (11). These rare heteromorph ammonites display the most stunning shell shapes (Fig. 1), generated by a combination of different modes of shell coiling during development. For a long time considered as “aberrant,” these forms have marveled and puzzled paleontologists for years. In addition to numerous taxonomic studies, special attention has been paid to the inference of their hydrostratic properties, lifestyle, and paleoecology

coiling | symmetry breaking | chirality | mathematical model | mollusk

**A**mong metazoans, Bilateria are organized along an antero-posterior and a dorso-ventral axis that both define the plane of bilateral symmetry and the left and right sides of the animal. Although bilaterian animals are externally mostly symmetric, they usually show a consistent left–right asymmetry in internal organs. How left–right symmetry is broken during development raises fundamental questions, such as the functional implications of asymmetry; defective left–right asymmetry leading to severe pathologies in humans; the developmental stage at which asymmetry is initiated; the dominance in most cases of a given direction (e.g., our heart most often to the left side, liver to the right) rather than a random 50/50 ratio; the extent to which left–right symmetry-breaking processes have been evolutionarily conserved among Bilateria; how multilevel asymmetries, from molecular, cellular, to organismal level, are related to each other; and how consistent asymmetry is generated in a world where no macroscopic process of chemistry or physics can be used to define unequivocally left from right (1–4).

In contrast to most Bilateria, snails display a conspicuous outward asymmetry manifested by a typically dextral (with an opening on the right side when the tip is up) or, rarely, sinistral helicospiral shell together with marked left–right anatomical asymmetries. The characteristic helicospiral shape of snail shells is a particular kind of chirality, a form being *chiral* if it cannot be superimposed on its mirror image, like our left and right hands. Shell chirality has intrigued biologists for centuries, and snails have emerged as model organisms to address the genetic and developmental bases of left–right symmetry breaking in Bilateria (5). Chirality in snails is in direct contrast with the shape of most

## Significance

**A theoretical model suggests that a mechanically induced twist of the soft body underlies the formation of helicospiral shells in snails and ammonites and also accounts for the startling and unique meandering shells observed in certain species. This theory addresses fundamental developmental issues of chirality and symmetry breaking: in the case of ammonites, how a bilaterally symmetric body can sometimes secrete a nonsymmetric shell; for gastropods, how an intrinsic twist possibly due to the asymmetric development of musculature can provide a mechanical motor for generating a chiral shell. Our model highlights the importance of physical forces in biological development and sheds light on shell coiling in snails, which have been used for a century as model organisms in genetic research.**

Author contributions: R.C. and D.E.M. conceived the study; A.G. and D.E.M. devised the mathematical model; D.E.M. performed computations; R.C. performed the comparative approach; D.E.M. collected data on shell coiling; and R.C., A.G., and D.E.M. contributed to the writing of the paper.

The authors declare no competing interest.

This article is a PNAS Direct Submission. N.H.L. is a guest editor invited by the Editorial Board.

Published under the [PNAS license](#).

See [online](#) for related content such as Commentaries.

<sup>1</sup>To whom correspondence may be addressed. Email: [regis.chirat@univ-lyon1.fr](mailto:regis.chirat@univ-lyon1.fr).

This article contains supporting information online at <https://www.pnas.org/lookup/suppl/doi:10.1073/pnas.2109210118/-DCSupplemental>.

Published November 22, 2021.

\*When we use the vernacular term “ammonites,” we refer to representatives of the cephalopod subclass Ammonoidea.



**Fig. 1.** Heteromorph ammonites with chiral shells. (A) *Turrillites costatus* (Cenomanian, France). (B) *Colchidites breistrofferi* (Barremian, Columbia); note the inner helicospiral shell followed by a planispiral stage. (C) *N. mirabilis* (Turonian, Japan). (D) Computed tomography scan of a *N. mirabilis* (Upper Cretaceous, Japan) showing the inner planispiral whorls. (E) *D. stevensoni* (Upper Cretaceous, United States). (F) Two enantiomorphs, sinistral and dextral, of *D. stevensoni* (Upper Cretaceous, United States). (Scale bars, 10 mm.) Specimen numbers are given in [SI Appendix](#), [Appendix B](#).

(12–14). However, a key question of developmental biology remains: What are the symmetry-breaking processes involved in the development of asymmetric shells among representatives of a group overwhelmingly characterized by a well-marked bilateral symmetry diagnostic of the cephalopod body plan?

The relative simplicity of the shell-growth process in mollusks—an accretionary process occurring at the current shell opening by the secreting mantle edge—and the diverse and distinct forms that are generated, as described above, make mollusks an excellent case study for investigating symmetry breaking during development, notably in light of recent progress made in developmental biology on this question in the model organism, the pond snail *Lymnaea*. Here, we present a comparative analysis between gastropods and ammonites and propose a unifying model of shell coiling based on the interaction of the animal's soft body with its secreted hard shell. Our model provides a physical explanation for how a bilaterally symmetric ammonite body may secrete, on occasion, an asymmetric shell and also addresses within the same framework the ubiquitous formation of helicospiral shells in gastropods, in light of the exception of bilaterally symmetric shells of limpets.

## 1. Background

**A. How Snails Got their Handedness.** A direction of shell coiling in snails is overwhelmingly predominant in a given species, with more than 90% of snails exhibiting dextral shells (15). For example, only six specimens of sinistral *Cerion* have ever been found among probably millions of specimens examined (16). Pond snails of the genus *Lymnaea* have become model organisms to study the genetic and developmental basis of left–right

asymmetry, leading to a model of maternal inheritance, in which offsprings' handedness is dictated by the mother's genotype (17, 18) by a single maternal locus (19). Gastropods display a spiral cleavage mode of early cell divisions, as do most representatives of the Lophotrochozoa (one of the three superphyla of Bilateria). The first sign of chirality in snails is distinguishable in the orientation of the cleavage planes, and handedness may be defined as early as in the first or second blastomere divisions. But temporal and spatial cytoskeletal dynamics for dextral and sinistral embryos are not mirror images of each other and show a bias toward dextral forms from the early stages of spiral cell division (20). Strikingly, inverting genetically specified third-cleavage directions by mechanically altering the relative orientation of cells leads to snails with inverted handedness, manipulated embryos growing to “dextralized” sinistral or “sinistralized” dextral snails (21). This handedness in cleavage acts upstream of the Nodal signaling pathway long known to be involved in left–right asymmetry in vertebrates and involved in snails, too (22). In the quest to discover the long-sought maternally expressed gene determining handedness, a diaphanous-related formin gene has been identified (23, 24), providing a proof for the role of an actin cytoskeleton-regulating protein in determining the arrangement of blastomeres. In summary, left–right asymmetry in snails' anatomy originates in cellular architecture. The dynamics of the inherently chiral cytoskeleton governs mechanically the asymmetric behavior of dividing cells at the earliest stage of development and, ultimately, the body- and shell-handedness. We will show, however, that if the link between spiral cleavage-, body-, and shell-handedness is obvious in the model organism *Lymnaea* (and probably many other gastropods), the link between cleavage pattern and helicospiral coiling itself is not straightforward and with a single explanation.

**B. Ammonites Took a Weird Turn.** In contrast to gastropods that display a spiral cleavage typical and ancestral of the molluscan phylum, cephalopods show a bilateral cleavage. In this case, the first cleavage furrow fixates the plane of bilateral symmetry of the animal, while the second furrow separates the future anterior and posterior areas (25). Moreover, unlike gastropods, a well-marked bilateral symmetry of the body organization both external and internal (e.g., symmetry and position of paired organs, such as gills or retractor muscles) is a diagnostic feature of the cephalopod body plan (26, 27). A bilateral symmetry also characterizes the shell of about 99% of ammonite genera, and though their soft body organization remains poorly known, muscle attachment marks are also bilaterally symmetric (28), unlike those of snails. We also know that the embryonic shell (ammonitella) is bilaterally symmetric (29), even in heteromorph ammonites with a postembryonic helicospiral shell (30, 31). Moreover, while chirality in snails is visible at the earliest embryonic stages, the shell of heteromorph ammonites only becomes chiral at a much later stage of development, sometimes well after hatching and organogenesis—i.e., well after the stage at which the anatomical symmetries are established. Note that we reserve the term “heteromorph” for species displaying a nonplanar shell, despite the fact that a number of bilaterally symmetric species (but with nonoverlapping whorls) have been called heteromorphs.

Heteromorph ammonites with helicospiral shells have evolved repeatedly from ancestors with bilaterally symmetric, planispiral shells (11, 32, 33). One particularly intriguing feature is the modifications of their shell symmetry during development (Fig. 1 B–F). For example, *Didymoceras*, shown in Fig. 1E, displays a bilaterally symmetric shell at the juvenile stage (straight or planispiral); a middle growth stage of asymmetric, helicospiral shell; and a bilaterally symmetric shell portion at maturity. Therefore, the shell shifts from bilaterally symmetric to asymmetric and then back to symmetric. It is difficult to conceive how the anatomical symmetry of the body itself could have shifted in

the same way during development. In fact, the morphology of the shell in *Didymoceras* (and genera of other families) shows that during the asymmetric part, the ventral side of the shell runs along the longer helicospiral and the dorsal side on the shorter one (which results in shell edge and ribs oblique to the growth direction), while the left and the right sides run along helicospirals of the same length, i.e., grow at the same rate as in planispiral shells, contrarily to gastropods, in which helicospiral shells display a clear left–right asymmetry in growth rate.

In contrast to snails, in which the direction of shell coiling is overwhelmingly predominant in a species, a study of about 1,500 specimens of *Didymoceras* shows roughly an equal percentage of dextral and sinistral shells (*Didymoceras stevensoni*,  $n = 264$ , dextral/sinistral [d/s] ratio: 47/53; *Didymoceras nebrascense*,  $n = 882$ , d/s ratio: 49/51; *Didymoceras cheyennense*,  $n = 338$ , d/s ratio: 52/48) (34). This roughly 50/50 ratio in handedness has also been reported in other genera of Nostoceratidae (35, 36), Heteroceratidae (37), or Turrilitidae (38), which suggests that the direction of asymmetry was randomly determined and nonheritable. Indeed, in the case of asymmetry induced by mechanical twisting, as will form the premise of our model, the twisting is equally likely to occur in either direction, and the actual observed directionality would be determined by “noise” in the system and thus be unpredictable and nonheritable. Likewise, in the known cases of existing Bilateria displaying a random direction of asymmetry in some anatomical traits, the direction of asymmetry is nonheritable (39).

The genus *Nipponites* displays some of the most startling shapes observed in Nature (Fig. 1 C and D). While it seems to be irregularly convoluted at first sight, it is not (40), and the shell actually follows a precise and reproducible developmental sequence. At juvenile stages, *Nipponites* has a planispiral, logarithmically coiled shell with nonoverlapping whorls. Then, the shell unfolds in a succession of meandering oscillations on each side of the plane of bilateral symmetry of the first planispiral stage, forming alternating dextral and sinistral helical sections of increasing wavelength and amplitude. We refer to this inversion of handedness as a *perversion*, following the nomenclature introduced by the mathematician Listing and used by Maxwell and d’Arcy Thompson (41–44). *Nipponites* is thought to derive from *Eubostrychoceras* (35), a genus that displays bilaterally symmetric planispiral whorls in the early stages, a middle growth stage with a helicospiral shell (dextral or sinistral in a 50/50 ratio), and a bilaterally symmetric shell segment at maturity. An important contribution in the geometric description of these heteromorph ammonites was made by Okamoto (45–47), who showed that these shapes could be modeled by varying the curvature and torsion of a centerline curve. However, this author assumed that shell coiling was controlled by the orientation of these ammonites in the water column through an unknown regulatory mechanism.

In summary, comparative data present us with a conundrum: Unlike snails, evidence suggests that ammonites had a bilaterally symmetric body diagnostic of the cephalopod body plan, but nevertheless sometimes secreted an asymmetric shell. Our goal here is to devise a mathematical model that can elucidate the developmental mechanism of shell coiling and symmetry breaking and show under what circumstances the different shell forms observed in ammonites and gastropods can be expected, under what conditions a symmetric body can give rise to an asymmetric shell, and how these asymmetric shells can change during development.

## 2. Model

Shell-building mollusks face strong geometric constraints associated with accretionary growth of their shell: They secrete during their development a shell to which the growing body will have to fit in subsequent stages sometimes several months or years

later. For instance, a mean shell growth rate of 0.061 mm/d in an immature *Nautilus* (48) implies that the rear of the growing body may be enclosed in a part of the shell tube secreted about 5 y earlier. Our main hypothesis is that any growth mismatch between the soft body and the secreted shell tube in which it resides can generate mechanical stresses balanced by an overall deformation of the body, impacting the geometry of future secretion. A mismatch between different growing parts of an organism plays a fundamental role in the genesis of mechanical forces underlying development and morphogenesis of plants and animals (49, 50), a mechanism involved in molluscan shell morphogenesis as well (8, 9, 51–54). That body growth and shell growth may be decoupled from each other is well known in bivalves and gastropods (55, 56). This question has rarely been addressed in *Nautilus*, though the allometric relationships between body and shell growth during sexual maturation has been reported in *Nautilus pompilius* (57). In ammonites, the allometric relationships between body and shell growth may be manifested by sometimes considerable variations in body-chamber length during development (28), which, however, did not prevent these animals from regulating their buoyancy, probably due to a flexibility of the mechanisms of buoyancy regulation, as in *Nautilus* (58). Our objective is to first investigate whether a mismatch between body and shell growth might account for the symmetry breaking observed in some ammonites and then to analyze whether the same methodology can consistently explain the helicospiral shell form in gastropods.

As shown in Fig. 2, we model the mollusk body by two elastic rods, one for the ventral side of the animal and one for the dorsal side. The reference shape of the growing body, i.e., the shape that the soft animal would take if it were removed from its shell, is given by the unstressed shape of these elastic rods, defined by their stress-free reference length and curvature that both evolve throughout development. For ammonites, the natural choice is to assume that the stress-free shape is a planar logarithmic spiral, for which the growth rates of the ventral and dorsal sides must be unequal: The ventral side is always growing at a higher rate than the dorsal side to ensure that they form a spiral. However, when the body occupies the shell, the elastic rods are constrained to match the shape of the shell tube that has been so far secreted. The shell shape is determined by both the orientation of the animal within the shell and the secretion rates. Naturally, the secretion rate on the ventral side is higher than on the dorsal side. If the secretion rates exactly match the body growth rates, then the shell shape will exactly match the logarithmic spiral shape of the body—in this case, the body is always in its reference shape, and no stress will be induced in the animal. If, however, the secretion rates do not exactly match the body growth rates, mechanical stress will be induced in the mollusk body, potentially forcing the body to twist within the shell to partially relieve these stresses (Fig. 2A; see also *SI Appendix, section 1*). If the animal twists within the shell, then the dorso-ventral axis will rotate about the centerline of the shell. Since the growth gradient follows the dorso-ventral axis, the axis about which the shell coils (dashed line in Fig. 2C) will also rotate, and thus the shell shape will change; in particular, any twist will, by construction, generate a nonplanarity to the centerline curve of the shell; i.e., twisting of the animal creates torsion<sup>†</sup> in the shell shape.

There is an interesting feedback at work: The shape of the shell that has been so far secreted dictates the stress in the animal within the tube; mechanical stresses generate a twist of the animal body; and the orientation of the animal dictates the subsequent shape of the shell, which will, in turn potentially create stresses on the growing animal. This two-way coupling between body shape and shell shape makes the problem particularly difficult to solve

<sup>†</sup>By torsion, we refer to the mathematical definition of a measure of the twisting out of the plane of curvature of a space curve.

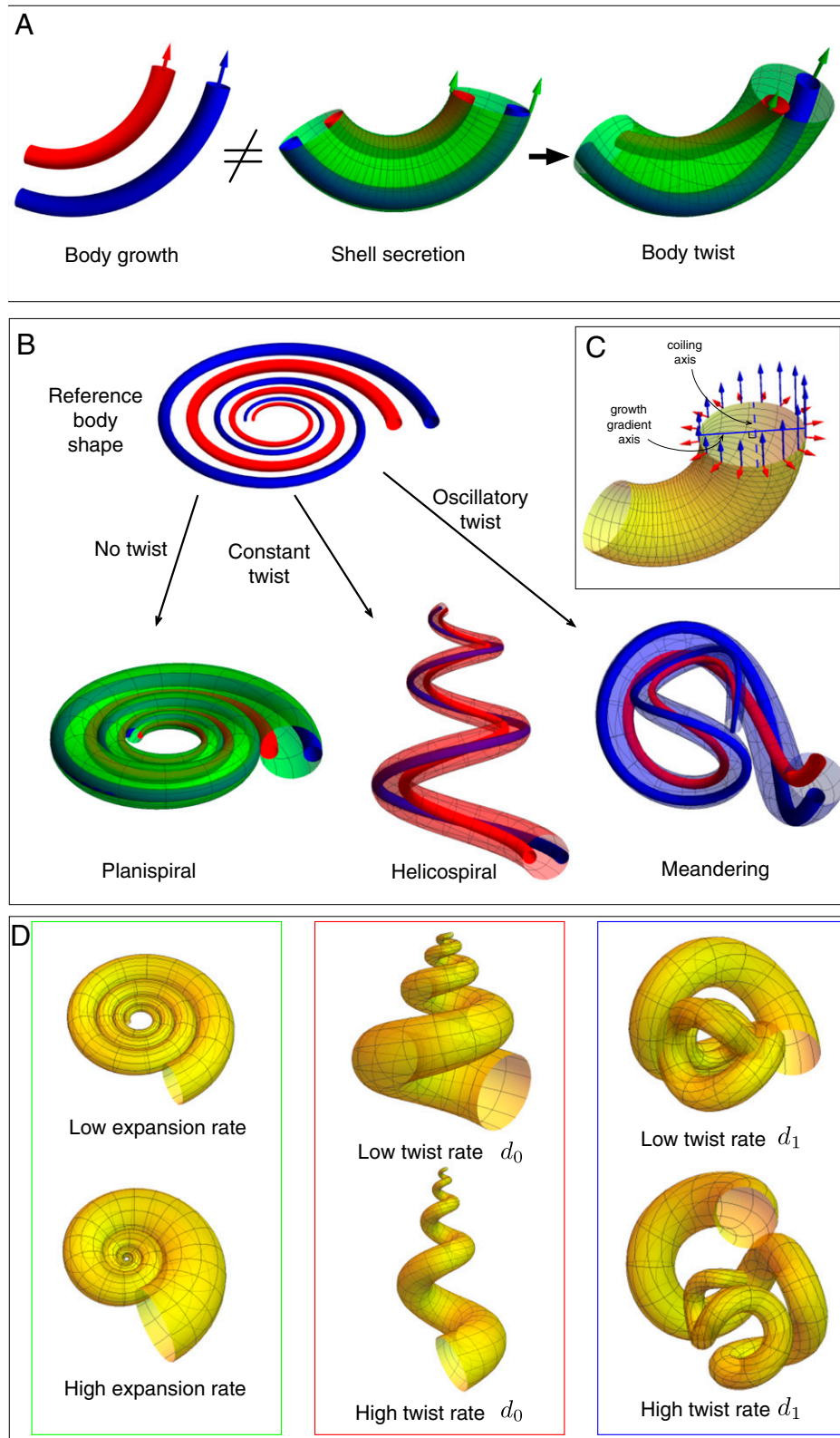


**Fig. 2.** Model schematic. (A) A mismatch between the growth rate of the body (idealized by dorsal and ventral elastic rods) and the secretion of the shell generates mechanical stress in the animal's body that may be partially alleviated by twisting of the body within the shell tube. (B) Three self-similar (i.e., with isometric growth) shell types may be generated from the same secretion parameters: if no twist, a planispiral shell; with constant twist, a helicospiral shell; and with oscillatory twist, a meandering shell. (C) Planar coiling geometry is captured by two parameters, an expansion rate  $c_1$  (red arrows) and a coiling gradient  $c_2$  (blue arrows). The coiling gradient (solid line) follows the dorso-ventral axis and generates coiling around the orthogonal axis (dashed line). (D) Representative shells for the three shell types.

in general. Here, our approach is to exploit self-similarity (i.e., isometric growth), which enables us to decouple the influence of mechanical stress on shell shape and to examine the conditions under which the animal may be predicted to secrete one of three classes of shell: 1) planispiral, 2) helicospiral, or 3) meandering. These three shell types can be produced with equivalent secretion rates, the only difference being the orientation of the secretion given by the twisting of the animal within the shell. In particular, there is no twist in the case of the planispiral shell, a constant twist rate (with respect to whorl) for the helicospiral, and an oscillatory twist rate in the case of the meandering shell (Fig. 2B). Therefore, assuming that the secretion rates and body-growth rates are given and that the only degree of freedom is the twisting, we can posit that the degree and form of twist by the animal will be the one that minimizes the mechanical energy of the contorted body, and thus the shell actually produced by the animal is the one corresponding to that energy-minimizing twist. With the assumption of self-similarity, we do not need to solve for the shape at each point in time based on the current orientation; rather, we find an energy-minimizing twist for a single (arbitrary) time point, and the self-similar assumption implies that the same twist will be selected throughout development.

The analysis above requires a description of the shell geometry, a characterization of the internal energy for the soft body, and a procedure for energy minimization. Full details are provided in *SI Appendix*; below, we briefly outline the modeling components.

**A. Geometry.** The geometry of the shell can be described by a set of only five parameters (*SI Appendix, section 2*),  $\{c_1, c_2, d_0, d_1, d_2\}$ , illustrated in Fig. 2 C and D. Here,  $c_1$  describes the aperture expansion rate,  $c_2$  describes the growth/secretion gradient—i.e., the difference in growth/secretion between the ventral and dorsal sides—that produces coiling, and the parameters  $d_i$  characterize twisting. In particular,  $d_0$  describes a constant twist, while  $d_1$  and  $d_2$  are, respectively, the amplitude and frequency of an oscillatory twist—equivalently, these correspond to an oscillation in the torsion of the shell centerline. In terms of these parameters, a planispiral shell corresponds to setting  $d_0 = d_1 = d_2 = 0$ ; a helicospiral shell is constructed by setting  $d_1 = d_2 = 0$ , with  $d_0 \neq 0$ ; and a meandering shell is constructed by setting  $d_0 = 0$ , with  $d_1$  and  $d_2$  both nonzero (in each case,  $c_1$  and  $c_2$  should be nonzero). Representative shells are shown in Fig. 2D, with parameters provided in *SI Appendix, section 2E*. In summary, the shell shape is characterized by one of the following parameter sets:

- Planispiral:  $S_p = \{c_1, c_2\}$
- Helicospiral:  $S_h = \{c_1, c_2, d_0\}$
- Meandering:  $S_m = \{c_1, c_2, d_1, d_2\}$

Our model is premised on the distinction between the geometry of the shell and the geometry of the body. When considering a bilaterally symmetric body, as with ammonites, the reference shape of the body is assumed to be planar, i.e., there is no intrinsic twist; thus, the body is described by only two parameters,  $\hat{S} = \{\hat{c}_1, \hat{c}_2\}$ , where we use the overhats to denote a reference quantity for the body. A mismatch between shell and body shape is then captured by any difference between  $\{c_1, c_2\}$  and  $\{\hat{c}_1, \hat{c}_2\}$ , while any twist of the body is described by the parameters  $\{d_0, d_1, d_2\}$ . However, another type of mismatch between body and shell may occur: The animal may be growing in such a way as to match the shell shape it is secreting, but at a faster or slower rate. This type of mismatch is accounted for by a scaling parameter  $\xi$  of arc length between the body and shell:

$$\hat{t} = \xi t, \quad [1]$$

where  $\hat{t}$  is the arc length of the centerline corresponding to the body,  $t$  is the arc length attached to the shell,  $\xi > 1$  means the

body is growing faster than the shell, and, conversely, for  $\xi < 1$ , the shell is growing faster.

**B. Mechanical Energy.** Given a set of parameters for both the shell and the body, we constrain the body to fit in the shell with the dorsal and ventral elastic rods situated on opposing sides of the shell tube and the ventral rod following the point of longest arc length. We then compute the mechanical energy in each of the rods by summing the energy contributions due to stretching, bending, and twisting (for details, see *SI Appendix, section 3*), employing a standard quadratic energy, with particular care required to account for the difference in arc length between the centerline of the shell tube and the ventral and dorsal sides.

**C. Energy Minimization.** Initially, we assume that the body growth and secretion rates are fixed through development for a given specimen, with the only degree of freedom being the twisting of the animal within the shell. This assumption is a sufficient and necessary condition for construction of a self-similar shell. Though we note that this is, at best, an approximation: The growth and secretion vary to some degree in most shells (we explore in Section E the consequence of a variation through development in these rates). Therefore, we fix the body parameters  $\hat{S} = \{\hat{c}_1, \hat{c}_2\}$ , the shell parameters  $\{c_1, c_2\}$ , and the stretch mismatch factor  $\xi$ . We also require defining the values of stiffness moduli  $\{K_1, K_2, K_3\}$ , which characterize the resistance to stretching, bending, and twisting of the body, respectively. The energy  $\mathcal{E}$  can then be expressed as a function only of twisting (*SI Appendix, section 3B*), i.e.

$$\mathcal{E} = \mathcal{E}(d_0, d_1, d_2).$$

For the planispiral shell, there is no twist, and the energy is  $\mathcal{E}_p = \mathcal{E}(0, 0, 0)$ . The helicospiral shell has energy  $\mathcal{E}_h(d_0) = \mathcal{E}(d_0, 0, 0)$ . As discussed in *SI Appendix, section 3C*, the most consistent approach to energy minimization is to fix  $d_2$ ; based on geometric considerations, we fix the oscillation frequency as  $d_2 = 0.8$  and define the meandering shell energy  $\mathcal{E}_m(d_1) = \mathcal{E}(0, d_1, 0.8)$ . The energy landscape is complex, varying both with the shell type and degree of mismatch imposed between body growth and secretion. Conceptually, the case that is of most interest is when the body growth rate exceeds the secretion rate, which causes the animal's body to be in compression. In this case, by examining the three components of the energy (*SI Appendix, section 3E*), a general trend emerges that shows there are values of the stiffness parameters  $K_i$  for which any of the three shell types can be an energy minimizer if sufficient compression is generated. The other case, secretion outpacing the body growth, requires the body to stretch during shell secretion; then, the body will be in tension, and in such cases, the planar shell was always found to be the energy minimizer.

To demonstrate this range of energy minimizers, we portray the energy landscape via a morphological phase space in Fig. 3, constructed by fixing the geometric parameters, with a small degree of imposed mismatch, then sweeping over a range of mechanical parameters and determining for each parameter choice the shell with the minimum energy. Two such plots appear in Fig. 3, with the energy-minimizing shell type denoted by color: green for planispiral, blue for meandering, and red for helicospiral. The coiling parameters  $\{\hat{c}_1, \hat{c}_2, c_1, c_2, \xi\}$  are chosen to correspond to sample values for a typical planispiral (Fig. 3A) and meandering (Fig. 3B) shell. We then sweep over the mechanical stiffness ratios  $K_1/K_2$  and  $K_3/K_2$ . For instance, a point in the lower right corner denotes a body with mechanical structure that has high resistance to stretching, but low resistance to twisting. In both cases, stiffness ratios exist for which each of the three shell types is predicted. In particular, when the parameters correspond to a typical planispiral shell, the planispiral shell type is the energy minimizer for most stiffness ratios, while when the coiling

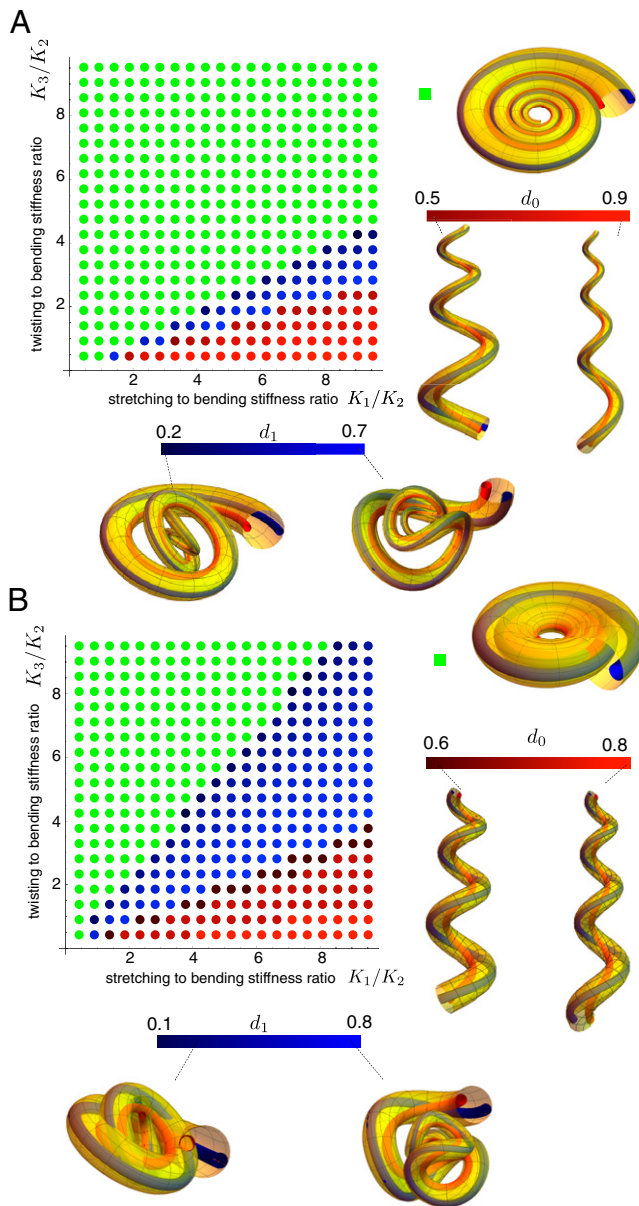


**Fig. 3.** Morphological phase space, sweeping over stiffness ratios  $K_1/K_2$  (stretching to bending) and  $K_3/K_2$  (twisting to bending). For each value of stiffness ratios, the energy-minimizing shell type—planispiral (green), helicospiral (red), or meandering (blue)—is computed, with energy-minimizing coiling values and corresponding shell forms indicated by the color bar. The shells in each phase space have equivalent coiling and expansion parameters, matching those in the planar green shell, differing only in the type and degree of twist. Body growth and secretion values are as follows:  $\hat{c}_1 = 0.02$ ,  $\hat{c}_2 = 0.2$ ,  $\hat{d}_0 = 0$ ,  $c_1 = 0.02$ ,  $c_2 = 0.25$ ,  $\xi = 1.0$  (A); and  $\hat{c}_1 = 0.02$ ,  $\hat{c}_2 = 0.323$ ,  $\hat{d}_0 = 0$ ,  $c_1 = 0.02$ ,  $c_2 = 0.4$ ,  $\xi = 1.0$  (B).

parameters correspond to sample values for a meandering shell (Fig. 3B) with two different coiling gradients, the heteromorph shell types are energy minimizers for a much wider range of parameter space.

It is important to note that we did not include the steric constraint that prohibits self-intersection of the shell tube with previous whorls. This means that some of the mechanically favorable shells are not geometrically possible. In particular, in Fig. 3B, the planispiral shell has significant overlap. While some degree of overlap is a feature found in almost all planispiral ammonites (Section 3), it is interesting to observe that with the secretion

rates such that the overlap leaves little room for the mollusk body in the planispiral shell tube, there is a significant increase in mechanical favorability of the twisted, nonoverlapping shells.

**D. Data Comparison.** Our model assumes that heteromorph ammonites emerge due to a mechanically induced twisting of the body, meaning that at the level of body growth and secretion, there is no difference between these shells and the far more typical planispiral ammonite. This feature enables us to test the model quantitatively: For each choice of coiling parameters  $\{\hat{c}_1, \hat{c}_2, c_1, c_2, \xi\}$ , we define the likelihood of finding a meandering or helicospiral shell by sweeping over possible stiffness ratios and determining the percentage of parameter space for which each shell type is an energy minimizer. Such a calculation appears in Fig. 4A. Here, we have set  $\hat{c}_1 = c_1$ ,  $\hat{c}_2 = c_2$ , and fixed  $\xi = 1.075$ , corresponding to an undersecreting shell (compressed body), but with body and shell shape matching. For each point in the  $c_1$ - $c_2$  plane, we compute the energy minimizer over a range of 100 values of stiffness ratios, using the same range as in Fig. 3. We then color that point with red, green, blue (RGB) value corresponding to the percentage of helicospiral (red), planispiral (green), and meandering (blue) energy minimizers. The dashed lines separate regions where each shell type is the overall winner. This plot gives an indication of where we would expect to find (and not find) meandering and helicospiral shells. In particular, the model predicts that coiling gradient is far more relevant than expansion rate, with meandering shells most likely in the coiling gradient range  $c_2 \in [0.4, 0.6]$  and helicospiral most likely for  $c_2 \lesssim 0.4$ , while for large coiling gradient, the planispiral shell is by far the most likely shape. To test these predictions, we have extracted the coiling parameters ( $c_1, c_2$ ) from a set of 19 meandering (*Nipponites mirabilis*) and 17 helicospiral (*Eubostrychoceras japonicum*) shells. These appear as the red and blue data points in Fig. 4A and show broad agreement with the model prediction. The best-fit shells for the indicated data points appear in Fig. 4B–E; shells (real and simulated) for all data points and all extracted parameter values are provided in [SI Appendix, section 4](#).

While Fig. 4 provides strong evidence in favor of the mechanical twisting hypothesis, we must be careful with its interpretation. It would be incorrect to conclude that planispiral ammonite shells are only likely to be found on the right side of the diagram, as, in fact, planispiral ammonites may be found over the entire range of the coiling parameters. Here, we emphasize that the twisting only occurs if there is a mismatch between body growth and shell secretion, characterized in this calculation by setting  $\xi = 1.075$ , meaning that the reference shape of the body is 7.5% longer than the shell tube it is secreting. Without some form of mismatch, the body is stress-free in the planar state, and, thus, the planispiral shell is always mechanically favorable. Even with a reduced mismatch, the regions in which meandering and helicospiral shells are predicted become much smaller: A sample morphospace with  $\xi$  decreased to 1.025 is shown as Fig. 4A, *Inset*; here, the planispiral shell is the most favorable shape for all values of coiling parameters. The model thus predicts that most ammonites secreted a planispiral shell due to low or no mismatch. It is for this reason that we do not include data points for planispiral shells in Fig. 4; the point of the computation is not to predict the presence of planispiral shells, but rather to predict where heteromorph shells will appear when the necessary ingredient of a mismatch is present.

**E. Varying Shell Type through Development.** Observe that the twisting parameters do not appear in Fig. 4. Thus, while the helicospiral and meandering shells occupy much of the same region of the coiling parameter space, the difference in form comes from the simple difference between a constant twist rate, in the case of the helicospiral shell, and an oscillatory twist, in the case of the meandering shell. It is worth highlighting that such distinctively

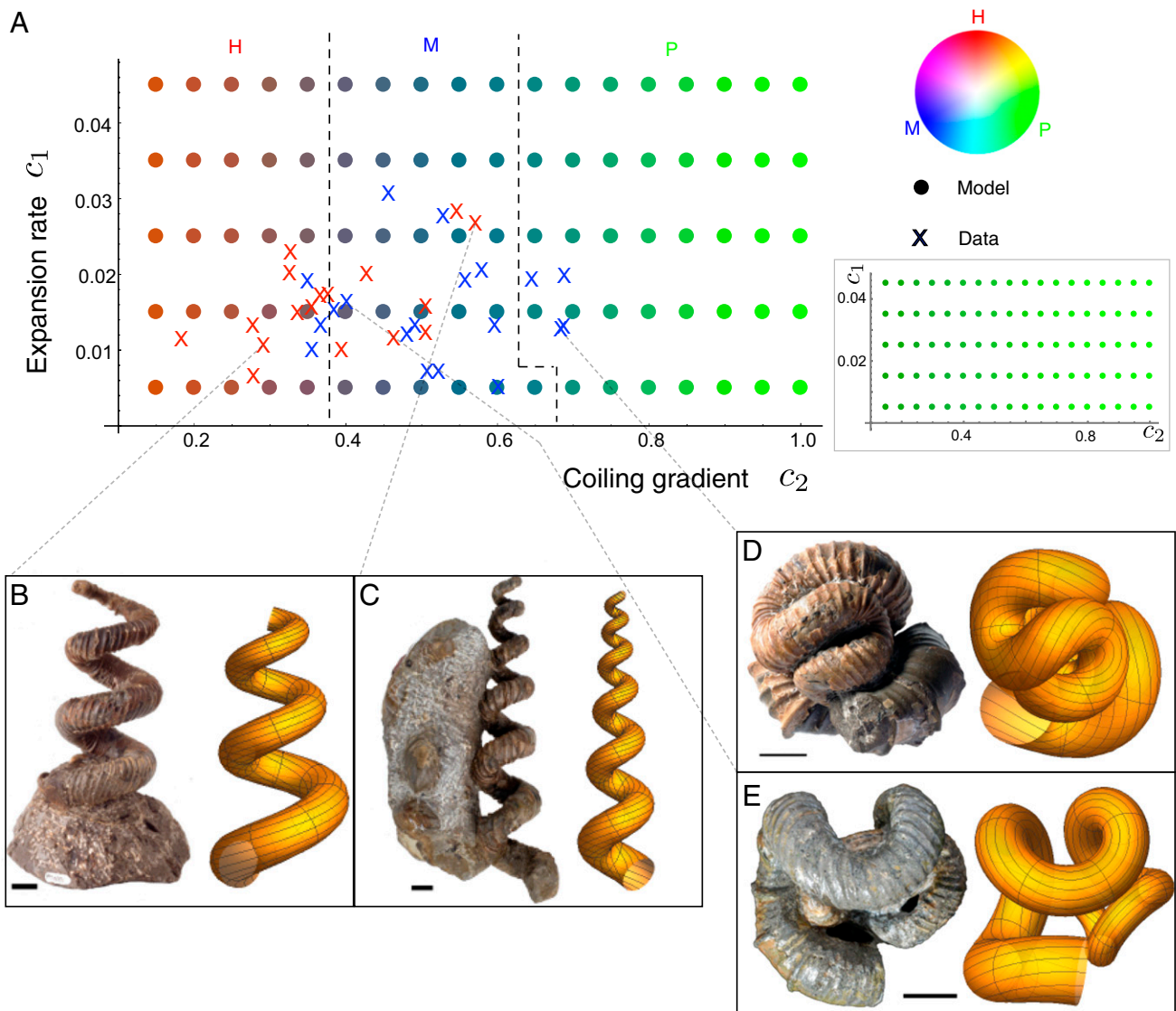


**Fig. 4.** (A) A phase space of coiling parameters is created by sweeping over mechanical stiffness ratios and computing the energy-minimizing shell, then coloring the point using RGB value corresponding to the percent of energy minimizers of each type—planispiral, green; helicospiral, red; meandering, blue. Data points for 19 meandering and 17 helicospiral shells are plotted using extracted coiling parameters. (A, *Inset*) A phase space with decreased compression factor. (B–E) Sample shell images and simulated shells with extracted parameters, corresponding to the indicated points (B and C, *E. japonicum*; D and E, *N. mirabilis*). (Scale bars, 10 mm.)

different forms may be mechanically favorable in the same region of this (two-dimensional) coiling space, which may explain why some shells display both types of coiling at different life stages (59) and why *Nipponites* shares many diagnostic characteristics with the coexistent *Eubostrychoceras*, from which it derives (35).

In our model, a transition in shell form can be generated by a change in mismatch and/or stiffness parameters during development. This is demonstrated in Fig. 5, in which we provide simulations of *D. nebrascense* (A) and *Nostoceras malagasyense* (B). The shell in Fig. 5A was obtained by first varying the arc-length mismatch parameter  $\xi$ , causing a transition in the juvenile stage from planispiral to meandering to helicospiral, and then varying the coiling and stiffness parameters in the late stage of development, which generates the reverse transition from helicospiral to meandering to planispiral (see details in *SI Appendix, section 5*). A similar transition produces the shell in Fig. 5B, though with the juvenile transition missing due to breakage in our specimen. Although we can only speculate on the biological significance of these parameter changes, it should be noted that shell-coiling changes in the last stages of development of many ammonites

are associated with sexual maturation, which, in *Nautilus*, is associated with modifications of growth of the shell and body parts (60). Our study of heteromorph ammonites illustrates also the clear difference between a purely geometric simulation of shell coiling and a model that includes explicitly developmental mechanisms and physical constraints. Indeed, while it is possible to simulate a developmental transition between a helicospiral and planispiral stage with coaxial coiling, our model shows that this coaxiality is mechanically unlikely. As evident in Figs. 3 and 4A and demonstrated more thoroughly in *SI Appendix, section 6*, the regions of parameter space in which the helicospiral and planispiral shells are mechanically favorable are always separated by a region in which the meandering shell is favorable. Therefore, if a change in shell type occurs during development due to a continuous change in parameters, our model predicts that a transition from helicospiral to planispiral must always pass through an intermediate meandering stage, which, by construction, will reorient the coiling axis. This rule is consistent with the fact that, to our knowledge, helicospiral and planispiral stages are never strictly coaxial in heteromorph ammonites; the coiling axes can

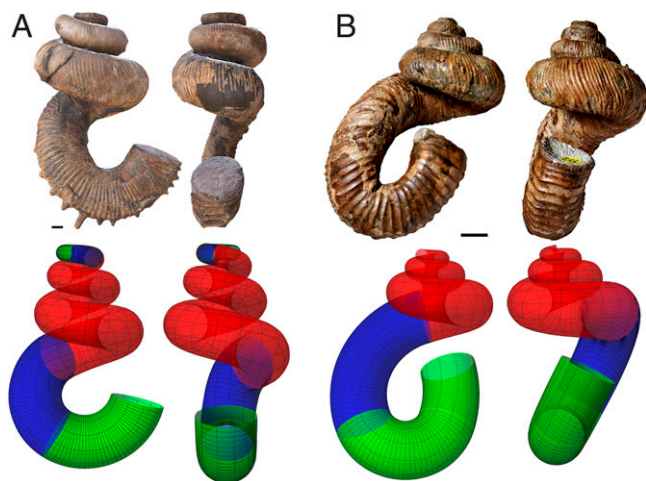


**Fig. 5.** Simulation and images of *D. nebrascense* (A) and *N. malagasyense* (B), obtained by varying the mismatch and stiffness parameters during development, causing transitions in development between planispiral (green), meandering (blue), and helicospiral (red). (Scale bars, 10 mm.) Shell specimen info and other model parameters are provided in [SI Appendix](#).

even be at right angles to each other (Fig. 1 B and E). This prediction is an example of a developmental constraint imposed by mechanics of morphogenesis (see ref. 9 for a discussion of this concept).

### 3. A Twist on Shell Coiling

Although heteromorph ammonites with chiral shells represent only about 1% of 3,000 genera, their geometric diversity surpasses that of the other ammonites, which probably lies in the fact that they have nonoverlapping whorls. In gastropods, a whorl partially dictates the growth path of the next overlapping whorl (61, 62). The mantle secretes an overlapping layer on the previous whorl, to which it adheres, and when this attachment zone is partially or totally lost, the coiling geometry is quantitatively modified (63). Whorl overlap played a role in ammonites too (64), and, in some way, constrained the range of possible morphologies in restricting the degrees of freedom of the growing system. For instance, a shell of the kind of *Didymoceras*, generated by a varying coiling geometry during development, could not be achieved with overlapping whorls. But, then, what are the regulation mechanisms of shell coiling in the nonoverlapping case?

Since mollusk shells are incrementally secreted along their opening edge, it seems logical that their coiling geometry could be fully understood in light of growth-regulating processes localized at the secreting mantle edge only. This idea has motivated all theoretical models of shell coiling and experimental approaches as well, but is confronted with an issue especially obvious in the case of heteromorph ammonites. One puzzling aspect of their morphogenesis is indeed the mechanisms that govern the three-dimensional path followed by the secreting mantle edge, resulting in highly convoluted forms. Theoretical models predict that an incremental rotation of the growing front underlies the development of helicospiral shells (45, 65, 66). Yet, to our knowledge, no mechanism localized at the mantle edge can trigger this movement. Our model suggests that this incremental rotation may be naturally triggered by a mechanical twist of the body, resulting from a mismatch between body and shell growth. An important conclusion may then be drawn from the study of these heteromorph ammonites: Although the form of the shell corresponds only to a spatiotemporal record of accretionary growth at its edge, the three-dimensional path followed by the secreting mantle edge is partly governed by the mechanics of the body inside the shell. Whereas it is now clear that some

ornamentation patterns in mollusk shells emerge as the result of mechanical forces at the secreting mantle margin (8, 9, 51–54), our study shows that the mechanical interactions between body and shell may also play a key role in the regulation of shell coiling.

This mechanical hypothesis explains a number of puzzling characteristics of these ammonites—notably, how they secreted asymmetric shells while keeping a bilaterally symmetric body diagnostic of cephalopods. With the same bilaterally symmetric growth gradient at the shell edge, an asymmetric or symmetric shell may be secreted, depending on whether the bilaterally symmetric body is twisted or not. This mechanical twist is recorded by the angular offset between the ventral siphuncle in the posterior part of the body chamber and the anterior ventral zone toward the shell edge (67). In a sinistral *Turrilites*, the ventral siphuncle is shifted toward the right side of the shell tube, while dorsal muscle scars are shifted toward the opposing left side (ref. 68, plate 18, figures 1–3). This mechanical twist also explains why asymmetric shells may develop after hatching, well after organogenesis and the formation of the plane of bilateral symmetry of the body. Further, the modifications of shell symmetry during development, such as the shifts seen in some genera from bilaterally symmetric to asymmetric and to symmetric again, reflect changes in mechanical strains affecting the bilaterally symmetric body. The fact that heteromorph ammonites with asymmetric shells have repeatedly evolved from ancestors with bilaterally symmetric shells is also consistent with this ahistorical generic mechanism.

In our model, the mechanical energy is equivalent for twisting in either direction. A twist of a bilaterally symmetric body is thus consistent with a random, nonheritable direction of shell-handedness, with right- and left-handed coiling arising with equal probability. However, representatives of the family Turrilitidae (Fig. 14) show another puzzling evolutionary trend, to our knowledge unique in the fossil record, and that may be interpreted in light of our approach. In the genus *Mariella* from South Africa and Texas, Albian species are dextral or sinistral in a 50/50 ratio, while all Cenomanian species are sinistral (38, 69). Thus, directional asymmetry arose from ancestors where left–right asymmetry was random. Similar evolutionary patterns in current phallostethid fishes and fiddler crabs have been interpreted as an “unconventional mode” of evolution (“phenotype precedes genotype”), the idea being that phenotypic variation (right- or left-handed) arose before genetic mechanisms controlling a given direction of asymmetry (39). But this interpretation depends on the way phenotypic characters are defined. Mechanical forces may generate helicospiral coiling, and though they are growth-dependent and modulated by genetic and molecular processes so that their outcome cannot be described as “phenotype first,” they may equiprobably produce dextral or sinistral forms. Directional asymmetry, on the other hand, requires a consistent bias toward one side, as in physical systems generating helices (70). In light of randomization of visceral asymmetry in mutant mice, an original two-component abstract system has been proposed to explain how left–right asymmetry might arise in Bilateria (71): A generic process (a reaction–diffusion system in the original hypothesis) producing random asymmetry at the cellular and multicellular level can be consistently biased toward a direction by a mechanism that converts molecular to cellular asymmetry. Likewise, the fixation of sinistral shells in Turilitidae can be interpreted in light of a two-component process: a generic, mechanical process generating helicospiral shells with no preferred handedness in ancestral forms and another one (that unfortunately will remain unknown) introducing a bias toward the leftward coiling in descendant species. An analogous situation has been described in the case of cardiac development in amniotes, in which a buckling instability twists the straight cardiac tube into a helical loop with random handedness, while molecular and cellular mechanisms introduce a bias that, except in rare mutants, consistently triggers a rightward looping (72).



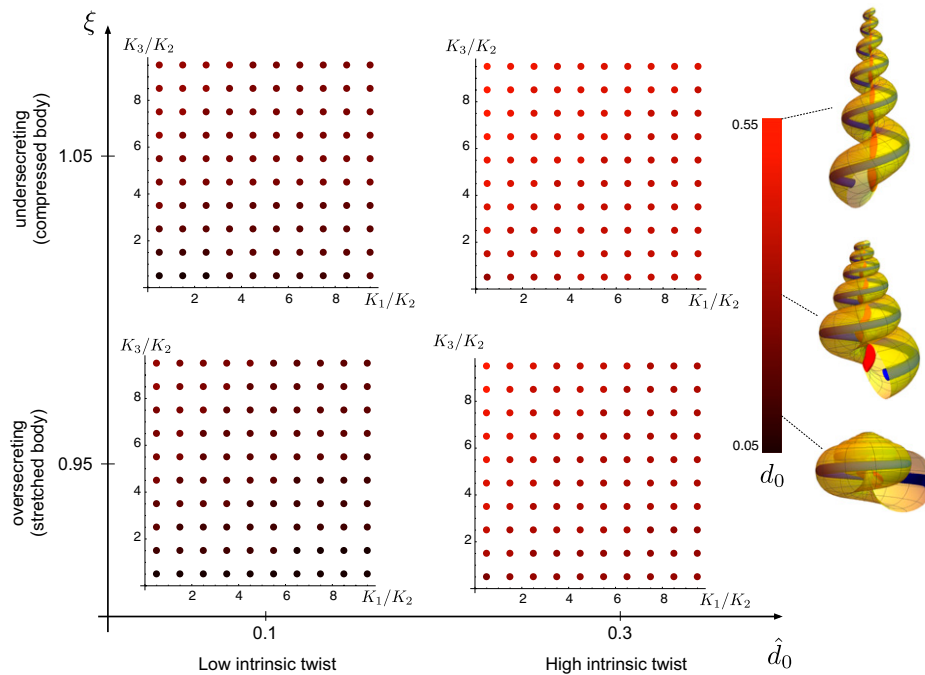


**Fig. 6.** Morphological phase space for gastropods for varying intrinsic twist  $\hat{d}_0 \in \{0.1, 0.3\}$  and mismatch parameter  $\xi \in \{0.95, 1.05\}$ , with a sweep over stiffness ratios  $K_1/K_2$  (stretching to bending) and  $K_3/K_2$  (twisting to bending) at each point. Energy-minimizing shell type is indicated by color, with red helicospiral shell the energy minimizer in every single case. Energy-minimizing twisting value  $d_0$  and corresponding shell type are indicated by the color bar. Body growth and secretion values are  $\hat{c}_1 = c_1 = 0.06$ ,  $\hat{c}_2 = c_2 = 0.9$ .

Finally, our approach may explain the development of rare Paleozoic nautiloids with helicospiral shells (73). It may also shed light on abnormal shell growth in ammonites with whorls overlapping, although the mechanical influence of this trait, probably dependent on the degree of overlapping, is not included in our model due to the additional theoretical difficulties that it would raise. In *Nautilus*, epizoans growing fixed on the outer surface of the shell may perturb the growth of the next whorl, slowing or inhibiting the forward movement of the animal's body (74), a process that could generate compression in the growing body. Our model suggests that this compression may generate meandering or helicospiral shells, similar to the abnormal forms described in slightly overlapping planispiral ammonites encrusted by epizoans (75).

#### 4. How Snails Coil their Shell

Much progress has been made on the genetic and molecular processes that set the left- or right-handedness of the asymmetric body in snails, but an important point rarely acknowledged is that the mechanisms underlying the development of helicospiral shells themselves remain poorly understood. First, the link between the body- and shell-handedness is not straightforward, contrarily to what may be reported in light of the development of the model organism, the pond snail *Lymnaea*. This genus is orthostrophic, which means that the body-handedness corresponds to the shell-handedness. But in hyperstrophic species, anatomically dextral animals have sinistral shell and vice versa, while in more complex cases called heterostrophy, shell-handedness changes after hatching (76). Moreover, although limpets show a dextral cleavage pattern and a right expression of *nodal* (22) and are right-handed in their body anatomy, both their embryonic and postembryonic shell is cone-shaped and bilaterally symmetric (77). The asymmetric development of gastropods is further complicated by a rotation that occurs during larval development and that moves the visceral mass, mantle, and shell at 180° with respect to the head and foot (this rotation is, confusingly, referred

to as “torsion” in the literature, but does not describe the coiling torsion of the shell). But this process cannot be unequivocally linked to helicospiral coiling since limpets also experience such a rotation (78). Furthermore, a left/right asymmetric gradient of the Dpp (decapentaplegic) protein (79) or an asymmetric cellular growth pattern in the mantle edge (80) cannot explain the incremental rotation of the growing front generating helicospiral shells. Comparative anatomy of limpets and helicospiral species suggests a possible mechanism.

In helicospiral species, the shell–muscle system is helically coiled around and anchored to the axial columella of the shell three-quarters to two whorls back from the aperture and extends into the foot (81). In cone-like limpets, muscle runs dorso-ventrally and attaches to the inner shell surface in a horseshoe-shaped muscle scar bilaterally symmetric on both sides of the body (82). While “true limpets” belong to the order Patellogastropoda, limpet-shaped shells have convergently evolved in not-closely-related species belonging to the four other gastropod orders predominantly helicospiral. In all cases, evolutionary changes from helicospiral to bilaterally symmetric limpet-shaped shells are correlated with a drastic modification of the shell–muscle system, from a coiled muscle attached on one side to the axial columella of the helicospiral shells to a horseshoe-shaped muscle bilaterally symmetric on both sides of the body typical of true limpets (82–84). These repeated modifications of both shell coiling and muscle–shell system during evolution suggest that both characters could be developmentally correlated and that bilateral asymmetry of the muscle–shell system could induce a twist of the body in species with helicospiral shells. Although this hypothesis remains to be tested experimentally, our theoretical framework already allows us to explore the effect of the intrinsic twist of the body on the shell form.

**A. Modeling Gastropod Form.** The observations above point to the possible role of intrinsic twist,  $\hat{d}_0$ . This parameter is geometrically

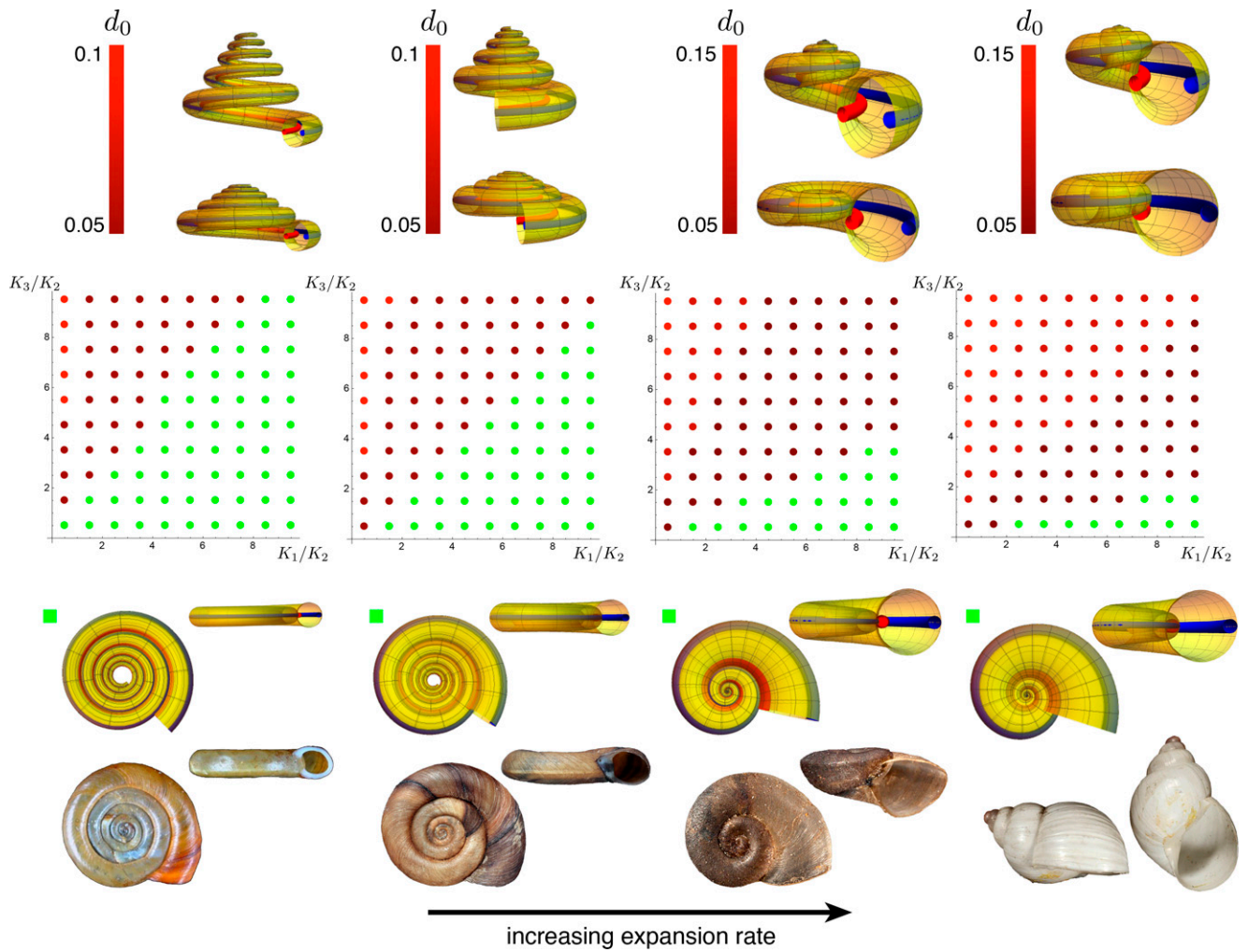


**Fig. 7.** A sequence of morphological phase spaces for varying expansion rate in the case of a low intrinsic twist ( $\hat{d}_0 = 0.1$ ) and stretched body ( $\xi = 0.95$ ) with energy-minimizing shells indicated by color. The model predicts an increased likelihood of planispiral shell at lower expansion rate, characteristic of trends in Planorbidae. Coiling parameters ( $c_1, c_2$ ) are, from left to right: (0.01, 0.2), (0.02, 0.37), (0.08, 0.48), and (0.1, 0.64). Shell images are (left to right): *Anisus leucostoma*, *Planorbis planorbis*, *Menetus dilatatus*, and *Bulinus albus*.

equivalent to the helicospiral shell parameter  $d_0$ , but is intrinsic to the animal's body. Due to the bilateral symmetry of ammonites,  $\hat{d}_0 = 0$  for all shells, while we explore in this section the mechanical consequences of  $\hat{d}_0 \neq 0$  for gastropods (note that anatomically, the blue rod is anterior and the red rod is posterior in the case of a gastropod). For given body parameters  $\{\hat{c}_1, \hat{c}_2, \hat{d}_0\}$  and secretion parameters  $\{c_1, c_2, \xi\}$ , we compute as before the effect of a mismatch by determining the energy-minimizing shell. The energy minimization proceeds in the same way as outlined above, with the appropriate variation to the twisting energy (*SI Appendix, section 7*). Naturally, in this case, if there is no mismatch, the animal will secrete a helicospiral shell that matches its helicospiral body shape. The question then is whether other shell types might be mechanically favorable, given a mismatch. To answer this question, we proceed as before, sweeping over a range of mechanical stiffness ratios and comparing the total mechanical energy in the planispiral shell with that of the helicospiral and meandering shells for which the energy is minimum. The result appears in Fig. 6. Here, we have fixed the coiling parameters and varied both the degree of mismatch via the parameter  $\xi$  and the degree of intrinsic twist via  $\hat{d}_0$  and plotted the resulting phase space. We find that in every single case, the helicospiral shell is the energy minimizer. We

have colored each point by the energy-minimizing twist value  $d_0$ , with sample shells appearing next to the color bar.

An analysis of different base-coiling parameters shows that the planispiral shell can also be the energy minimizer, but only in cases of a stretched body, whereas meandering shells are never found to be favorable (*SI Appendix, section 7*). In Fig. 7, we show the morphological phase space in the case of low intrinsic twist and  $\xi = 0.95$  (stretched body) for coiling parameters matching Planorbidae, a small-sized aquatic pulmonate gastropod family. As shown in Fig. 7, the model predicts a greater likelihood of planispiral shells at low expansion rate, with the helicospiral shell being the dominant form at higher expansion rate. This trend in variation is consistently observed among Planorbidae and was already described in 1867 in the first phylogenetic tree based on fossil evidence (85), just 8 y after Darwin's Origin of Species. Comparing Figs. 3 and 7 also highlights an interesting mechanical duality: Tension can cause an asymmetric body to take on a symmetric shape, while compression can cause a symmetric body to take an asymmetric shape.

Our mechanical model predicts that in the presence of an intrinsic body twist, helicospiral shells are strongly favored. It is well known that, once pulled out of its helicospiral shell, the body of gastropods remains helicospiral. This might seem logical since the body has grown and had to fit inside the shell. We suggest,

however, that the body is helicospiral because it is intrinsically twisted, possibly due to the asymmetric development of the muscle–shell system, and that this intrinsic twist provides the motor for the incremental rotation of the secreting mantle edge required to generate the helicospiral shell.

Our approach may help to explain many aspects of shell coiling that are difficult to interpret in terms of relative growth rates at the shell edge only, such as the development of hyperstrophic or heterostrophic species (76), of heteromorph snails involving a rotation of the body inside the shell (86), of pharmaceutically induced “banana-shaped” Planorbidae (87), or of abnormal helicospiral individuals of this family found in the wild (63), among other examples. Further, our study may inform the long-standing debate about the assignment of Bellerophonitida to gastropods (88, 89). These constitute an extinct order of mollusk of uncertain systematic position (Cambrian–Triassic) characterized by a planispiral, rapidly expanding shell, but interestingly displaying a pair of muscle scars symmetric on both sides of the shell (90), suggesting an untwisted body.

## 5. Conclusion

The natural world is overflowing with strikingly regular spiral, helical, and helicospiral shapes, such as keratin fibers, collagen assembly, DNA molecules, spiral bacteria, tendrils, climbing vines, seed pods, sheep horn, the cochlea, and umbilical cords, among others (70, 91–96). Such structures often develop as the result of fundamental mechanical forces generated by a mismatch between different parts (97–99). While most previous theoretical or experimental approaches have tried to relate global shell geometry only to the growth occurring at the shell edge, our study highlights how the position and mechanics of the body inside the shell can serve to regulate its morphogenesis. Through consideration of the orientation and mechanical energy of the soft body constrained by the shell in which it resides, we have identified a basic physical mechanism that explains the origin and diversity in form of shell coiling in mollusks. This includes, in the case of ammonites, a natural explanation for the development of an asymmetric shell by a bilaterally symmetric

animal and, in the case of gastropods, a mechanical motor for the generation of helicospiral shells due to an intrinsic twist possibly connected to the asymmetric development of musculature. Our model also explains the meandering shells of *Nipponites*, one of the most startling forms in Nature. It would be tempting to see in this unique morphology an arbitrary quirk of evolution. In fact, similar geometric forms consisting of alternating helical sections of opposite-handedness separated by multiple perversions are known to occur in bacterial shape and flagella, cellulose fibers, vine tendrils, and also telephone cords due to a combination of curvature-induced instability and geometric constraints (44, p. 150). In our study, the meandering form of *Nipponites* emerges as the energetically favorable path of an oscillatory twist of the animal's body in the shell. As ammonites have been extinct for 66 million years, it is, of course, impossible to confirm with certainty their body symmetry. However, as we have shown that it is mechanically unfavorable for an animal with an asymmetric body to secrete a symmetric or meandering shell, our study provides strong evidence for a bilaterally symmetric body, including in these heteromorph ammonites; this highlights the potential value of mechanics in deciphering the form of the soft body parts of a long-extinct animal. Likewise, snails, which have long been used as model organisms for genetic studies, could also constitute an excellent model for studying the canalizing role of mechanics in the genesis, variation, and evolution of biological forms.

**Data Availability.** A Mathematica notebook containing model details and calculations has been deposited in the Oxford University Research Archive (<https://doi.org/10.5287/bodleian:1ama4o2OZ>) (100).

**ACKNOWLEDGMENTS.** We are grateful to the people who provided us access to paleontological data: E. Robert, C. Salaviale (Université [Univ.] Lyon 1), F. Giraud (Univ. Grenoble), D. Berthet (Musée [Mus.] confluences), H. Châtelier (ammonites.fr), C. Scheskie (Denver Museum of Nature and Science), S. Luallin, S. Jorgensen (Western Interior Paleontological [Pal.] Society [Soc.]), C. Chen (Japan Agency for Marine–Earth Science and Technology), D. Aiba (Mikasa Museum), Y. Shigeta (National Museum of Nature and Science), H. Maeda, Y. Ito (Kyushu University Museum), Y. Shiino (Pal. Soc. Japan), and C. Serra (Museum CosmoCaixa). This work was supported by Engineering and Physical Sciences Research Council Grant EP/R020205/1.

1. L. N. Vandenberg, J. M. Lemire, M. Levin, It's never too early to get it Right: A conserved role for the cytoskeleton in left-right asymmetry. *Commun. Integr. Biol.* **6**, e27155 (2013).
2. M. Inaki, J. Liu, K. Matsuno (2016) Cell chirality: Its origin and roles in left–right asymmetric development. *Philos. Trans. R. Soc. Lond. B, Biol. Sci.* **371**, 20150403.
3. G. Lebreton *et al.*, Molecular to organismal chirality is induced by the conserved myosin 1D. *Science* **362**, 949–952 (2018).
4. T. Juan *et al.*, Myosin1D is an evolutionarily conserved regulator of animal left-right asymmetry. *Nat. Commun.* **9**, 1–12 (2018).
5. A. Davison, Flipping shells! Unwinding LR asymmetry in mirror-image molluscs. *Trends Genet.* **36**, 189–202 (2020).
6. B. Westermann, H. Schmidtberg, K. Beuerlein, Functional morphology of the mantle of *Nautilus pompilius* (Mollusca, Cephalopoda). *J. Morphol.* **264**, 277–285 (2005).
7. D. J. Jackson *et al.*, A rapidly evolving secretome builds and patterns a sea shell. *BMC Biol.* **4**, 1–10 (2006).
8. D. E. Moulton, A. Goriely, R. Chirac, The morpho-mechanical basis of ammonite form. *J. Theor. Biol.* **364**, 220–230 (2015).
9. A. Erlich, D. E. Moulton, A. Goriely, R. Chirac, Morphomechanics and developmental constraints in the evolution of ammonites shell form. *J. Exp. Zool. B Mol. Dev. Evol.* **326**, 437–450 (2016).
10. C. W. Wright, *Cretaceous Ammonoidea. Part I. Mollusca* (Treatise on Invertebrate Paleontology, Geological Society of America, Boulder, CO, Revised ed., 1996), vol. 4.
11. J. Wiedmann, The heteromorphs and ammonoid extinction. *Biol. Rev. Camb. Philos. Soc.* **44**, 563–602 (1969).
12. N. H. Landman *et al.*, Methane seeps as ammonite habitats in the US western interior seaway revealed by isotopic analyses of well-preserved shell material. *Geology* **40**, 507–510 (2012).
13. D. J. Peterman, M. M. Yacobucci, N. L. Larson, C. Ciampaglio, T. Linn, A method to the madness: Ontogenetic changes in the hydrostatic properties of *Didymoceras* (Nostoceratidae: Ammonoidea). *Paleobiology* **46**, 237–258 (2020).
14. D. J. Peterman, T. Mikami, S. Inoue, The balancing act of *Nipponites mirabilis* (Nostoceratidae, Ammonoidea): Managing hydrostatics throughout a complex ontogeny. *PLoS One* **15**, e0235180 (2020).
15. F. Van Batenburg, E. Gittenberger, Ease of fixation of a change in coiling: Computer experiments on chirality in snails. *Heredity* **76**, 278–286 (1996).
16. S. J. Gould, N. D. Young, B. Kasson, The consequences of being different: Sinistral coiling in cerion. *Evolution* **39**, 1364–1379 (1985).
17. A. H. Sturtevant, Inheritance of direction of coiling in *Limnaea*. *Science* **58**, 269–270 (1923).
18. G. Freeman, J. W. Lundelius, Evolutionary implications of the mode of D quadrant specification in coelomates with spiral cleavage. *J. Evol. Biol.* **5**, 205–247 (1992).
19. Y. Hosoi, Y. Harada, R. Kuroda, Construction of a backcross progeny collection of dextral and sinistral individuals of a freshwater gastropod, *Lymanea stagnalis*. *Dev. Genes Evol.* **213**, 193–198 (2003).
20. Y. Shibazaki, M. Shimizu, R. Kuroda, Body handedness is directed by genetically determined cytoskeletal dynamics in the early embryo. *Curr. Biol.* **14**, 1462–1467 (2004).
21. R. Kuroda, B. Endo, M. Abe, M. Shimizu, Chiral blastomere arrangement dictates zygotic left–right asymmetry pathway in snails. *Nature* **462**, 790–794 (2009).
22. C. Grande, N. H. Patel, Nodal signalling is involved in left–right asymmetry in snails. *Nature* **457**, 1007–1011 (2009).
23. A. Davison *et al.*, Formin is associated with left–right asymmetry in the pond snail and the frog. *Curr. Biol.* **26**, 654–660 (2016).
24. M. Abe, R. Kuroda, The development of CRISPR for a mollusc establishes the formin *Lsdia1* as the long-sought gene for snail dextral/sinistral coiling. *Development* **146**, dev175976 (2019).
25. S. Boletzky, Cephalopod development and evolutionary concepts. *Mollusca* **12**, 185–202 (1988).
26. S. Shigeno, S. Takeno, S. Boletzky, “The origins of cephalopod body plans: A geometrical and developmental basis for the evolution of vertebrate-like organ systems” in *Cephalopods—Present and Past*, K. Tanabe, Y. Shigeta, T. Sasaki, H. Hirano, Eds. (Tokai University Press, Tokyo), 23–34 (2010).
27. R. Hanlon, M. Vecchione, L. Alcock, *Octopus, Squid, and Cuttlefish: A Visual, Scientific Guide to the Oceans' Most Advanced Invertebrates* (University of Chicago Press, Chicago, 2018).
28. L. A. Doguzhaeva, R. H. Mapes, “The body chamber length variations and muscle and mantle attachments in ammonoids” in *Ammonoid Paleobiology: From Anatomy to Ecology*, C. Klug, D. Korn, K. De Baets, I. Kruta, R. H. Mapes, Eds. (Topics in Geobiology, Springer, Dordrecht, Netherlands, 2015), vol. **43**, pp. 545–584.
29. N. H. Landman, K. Tanabe, Y. Shigeta, “Ammonoid embryonic development” in *Ammonoid Paleobiology*, N. H. Landman, K. Tanabe, R. A. Davis, Eds. (Topics in Geobiology, Springer, New York, 1996), vol. **13**, pp. 343–405.

30. K. Tanabe, I. Obata, M. Futakami, Early shell morphology in some Upper Cretaceous heteromorph ammonites. *Trans. Proc. Paleontol. Soc. Japan N. Ser.* **124**, 215–234.
31. V. Druschits, The structure of the ammonitella and the direct development of ammonites. *Paleontol. J.* **2**, 188–199 (1977).
32. N. Monks, Cladistic analysis of Albian heteromorph ammonites. *Palaeontology* **42**, 907–925 (1999).
33. R. Hoffmann et al., Recent advances in heteromorph ammonoid palaeobiology. *Biol. Rev. Camb. Philos. Soc.* **96**, 576–610 (2021).
34. W. J. Kennedy, N. Landman, W. A. Cobban, G. Scott, Late Campanian (Cretaceous) heteromorph ammonites from the Western interior of the United States. *Bull. Am. Mus. Nat. Hist.* **2000**, 1–86 (2000).
35. T. Okamoto, Comparative morphology of Nipponites and Eubostriochoceras (cretaceous nostoceratids). *Trans. Proc. Paleontol. Soc. Japan N. Ser.*, **154**, 117–139 (1989).
36. H. C. Klinger, W. J. Kennedy, W. E. Grulke, New and little-known Nostoceratidae and Diplomoceratidae (Cephalopoda: Ammonoidea) from Madagascar. *Afr. Nat. History* **3**, 89–115 (2007).
37. H. C. Klinger, M. V. Kakabadze, W. J. Kennedy, Upper Barremian (Cretaceous) heteroceratid ammonites from South Africa and the Caucasus and their palaeobiogeographic significance. *J. Molluscan Stud.* **50**, 43–60 (1984).
38. H. Klinger, W. Kennedy, Turritulitidae (Cretaceous Ammonoidea) from South Africa, with a discussion of the evolution and limits of the family. *J. Molluscan Stud.* **44**, 1–48 (1978).
39. A. R. Palmer, Symmetry breaking and the evolution of development. *Science* **306**, 828–833 (2004).
40. H. Yabe, Cretaceous Cephalopoda from the Hokkaido. Part 2. Turritulites, Helicoceras, Heteroceras, Nipponites, Olcostephanus, Desmoceras, Hauericeras, and an undetermined genus. *Hokkaido J. Tokyo* **20**, 1–45 (1904).
41. J. B. Listing, Vorstudien zur Topologie (Vandenhoeck und Ruprecht, Göttingen, 1848).
42. W. E. L. G. Clark, P. B. Medawar, *Essays on Growth and Form Presented to D'Arcy Wentworth Thompson* (Oxford University Press, Oxford, UK, 1945).
43. J. C. Maxwell, *A Treatise on Electricity and Magnetism* (Clarendon, Oxford, UK, 1892).
44. A. Goriely, *The Mathematics and Mechanics of Biological Growth* (Springer Verlag, New York, 2017).
45. T. Okamoto, Analysis of heteromorph ammonoids by differential geometry. *Palaeontology* **31**, 35–52 (1988).
46. T. Okamoto, Changes in life orientation during the ontogeny of some heteromorph ammonoids. *Palaeontology* **31**, 281–294 (1988).
47. T. Okamoto, Developmental regulation and morphological saltation in the heteromorph ammonite *Nipponites*. *Paleobiology* **14**, 272–286 (1988).
48. A. J. Dunstan, P. D. Ward, N. J. Marshall, *Nautilus pompilius* life history and demographics at the Osprey Reef Seamount, Coral Sea, Australia. *PLoS One* **6**, e16312 (2011).
49. D. Ambrosi et al., Growth and remodelling of living tissues: Perspectives, challenges and opportunities. *J. R. Soc. Interface* **16**, 20190233 (2019).
50. O. Hamant, T. E. Saunders, Shaping organs: Shared structural principles across kingdoms. *Annu. Rev. Cell Dev. Biol.* **36**, 385–410 (2020).
51. R. Chirat, D. E. Moulton, A. Goriely, Mechanical basis of morphogenesis and convergent evolution of spiny seashells. *Proc. Natl. Acad. Sci. U.S.A.* **110**, 6015–6020 (2013).
52. A. Erlich, R. Howell, A. Goriely, R. Chirat, D. Moulton, Mechanical feedback in seashell growth and form. *ANZIAM J.* **59**, 581–606 (2018).
53. S. Rudraraju, D. E. Moulton, R. Chirat, A. Goriely, K. Garikipati, A computational framework for the morpho-elastic development of mollusk shells by surface and volume growth. *PLoS Comput. Biol.* **15**, e1007213 (2019).
54. D. E. Moulton, A. Goriely, R. Chirat, Mechanics unlocks the morphogenetic puzzle of interlocking bivalved shells. *Proc. Natl. Acad. Sci. U.S.A.* **117**, 43–51 (2020).
55. D. E. Lewis, R. M. Cerrato, Growth uncoupling and the relationship between shell growth and metabolism in the soft shell clam *Mya arenaria*. *Mar. Ecol. Prog. Ser.* **158**, 177–189 (1997).
56. P. E. Bourdeau, F. Johansson, Predator-induced morphological defences as by-products of prey behaviour: A review and prospectus. *Oikos* **121**, 1175–1190 (2012).
57. S. Hayasaka, K. Oki, K. Tanabe, T. Saisho, A. Shinomiya, "On the habitat of *Nautilus pompilius* in Tanon Strait (Philippines) and the Fiji Islands" in *Nautilus The Biology and Paleobiology of a Living Fossil*, W. B. Saunders, N. H. Landman Eds. (Topics in Geobiology, Springer, Dordrecht, Netherlands, 2010), vol. 6, pp. 179–200.
58. P. D. Ward, *The Natural History of Nautilus* (Allen & Unwin, Crows Nest, Australia, 1987).
59. T. Matsumoto, Some heteromorph ammonites from the Cretaceous of Hokkaido. *Mem. Fac. Sci., Kyushu Univ. Ser. D. Geol.* **23**, 303–366 (1977).
60. D. Collins, P. D. Ward, "Adolescent growth and maturity in *Nautilus*" in *Nautilus The Biology and Paleobiology of a Living Fossil*, W. B. Saunders, N. H. Landman Eds. (Topics in Geobiology, Springer, Dordrecht, Netherlands, 2010), vol. 6, pp. 421–432.
61. J. Hutchinson, Control of gastropod shell shape; the role of the preceding whorl. *J. Theor. Biol.* **140**, 431–444 (1989).
62. A. G. Checa, A. P. Jiménez-Jiménez, P. Rivas, Regulation of spiral coiling in the terrestrial gastropod *Sphincterochila*: An experimental test of the road-holding model. *J. Morphol.* **235**, 249–257 (1998).
63. C. Clewing, F. Riedel, T. Wilke, C. Albrecht, Ecophenotypic plasticity leads to extraordinary gastropod shells found on the "Roof of the World". *Ecol. Evol.* **5**, 2966–2979 (2015).
64. T. Ubukata, K. Tanabe, Y. Shigeta, H. Maeda, R. H. Mapes, Piggyback whorls: A new theoretical morphologic model reveals constructional linkages among morphological characters in ammonoids. *Acta Palaeontol. Pol.* **53**, 113–128 (2008).
65. D. E. Moulton, A. Goriely, R. Chirat, Mechanical growth and morphogenesis of seashells. *J. Theor. Biol.* **311**, 69–79 (2012).
66. D. E. Moulton, A. Goriely, Surface growth kinematics via local curve evolution. *J. Math. Biol.* **68**, 81–108 (2014).
67. P. Ward, Functional morphology of cretaceous helically-coiled ammonite shells. *Paleobiology* **5**, 415–422 (1979).
68. G. C. Crick, On the muscular attachment of the animal to its shell in some fossil Cephalopoda (Ammonoidea). *Trans. Linn. Soc. Lond. 2nd Ser. Zoology* **7**, 71–113 (1898).
69. D. L. Clark, Heteromorph ammonoids from the Albian and Cenomanian of Texas and adjacent areas. *Geol. Soc. Am.* **95**, 99 (1965).
70. S. Armon, E. Efrati, R. Kupferman, E. Sharon, Geometry and mechanics in the opening of chiral seed pods. *Science* **333**, 1726–1730 (2011).
71. N. A. Brown, L. Wolpert, The development of handedness in left/right asymmetry. *Development* **109**, 1–9 (1990).
72. A. Desgrange, J. F. Le Garrec, S. M. Meilhac, Left-right asymmetry in heart development and disease: Forming the right loop. *Development* **145**, dev162776 (2018).
73. C. Teichert et al., *Treatise on Invertebrate Paleontology: Part K Mollusca 3. Cephalopoda General Features—Endoceratoidea—Actinoceratoidea—Nautiloidea—Bactritoidea*. (The Paleontology Institute, Lawrence, KS, 1964).
74. J. Arnold, Shell growth, trauma, and repair as an indicator of life history for *Nautilus*. *Veliger* **27**, 386–396 (1985).
75. A. G. Checa, T. Okamoto, H. Keupp, Abnormalities as natural experiments: A morphogenetic model for coiling regulation in planispiral ammonites. *Paleobiology* **28**, 127–138 (2002).
76. T. Okumura et al., The development and evolution of left-right asymmetry in invertebrates: Lessons from *Drosophila* and snails. *Dev. Dyn.* **237**, 3497–3515 (2008).
77. M. C. Kay, R. B. Emler, Laboratory spawning, larval development, and metamorphosis of the limpets *Lottia digitalis* and *Lottia asmi* (Patellogastropoda, Lottiidae). *Invertebr. Biol.* **121**, 11–24 (2002).
78. A. Wanninger, B. Ruthensteiner, G. Haszprunar, Torsion in *Patella caerulea* (Mollusca, Patellogastropoda): Ontogenetic process, timing, and mechanisms. *Invertebr. Biol.* **119**, 177–187 (2000).
79. K. Shimizu et al., Left-right asymmetric expression of DPP in the mantle of gastropods correlates with asymmetric shell coiling. *Evodevo* **4**, 1–7 (2013).
80. A. B. Johnson, N. S. Fogel, J. D. Lambert, Growth and morphogenesis of the gastropod shell. *Proc. Natl. Acad. Sci. U.S.A.* **116**, 6878–6883 (2019).
81. R. M. Price, Columellar muscle of neogastropods: Muscle attachment and the function of columellar folds. *Biol. Bull.* **205**, 351–366 (2003).
82. J. Heller, *Sea Snails. A Natural History* (Springer, Cham, Switzerland, 2015).
83. L. Yamamori, M. Kato, Morphological and ecological adaptation of limpet-shaped top shells (Gastropoda: Trochidae: Fossarininae) to wave-swept rock reef habitats. *PLoS One* **13**, e0197719 (2018).
84. R. Tseng, B. A. Dayrat, Anatomical redescription of the limpet-like marine pulmonate *Trimusculus reticulatus* (Sowerby, 1835). *Veliger* **51**, 194–207 (2014).
85. M. W. Rasser, Darwin's dilemma: The Steinheim snails' point of view. *Zoosyst. Evol.* **89**, 13–20 (2013).
86. T.-S. Liew, A. C. M. Kok, M. Schilthuis, S. Urdu, On growth and form of irregular coiled-shell of a terrestrial snail: *Plectostoma concinnum* (Fulton, 1901) (Mollusca: Caenogastropoda: Diplommatinidae). *PeerJ* **2**, e383 (2014).
87. A. Baynes et al., Early embryonic exposure of freshwater gastropods to pharmaceutical 5-alpha-reductase inhibitors results in a surprising open-coiled "banana-shaped" shell. *Sci. Rep.* **9**, 16439 (2019).
88. W. F. Ponder, D. R. Lindberg, Towards a phylogeny of gastropod molluscs: An analysis using morphological characters. *Zool. J. Linn. Soc.* **119**, 83–265 (1997).
89. P. Bouchet, J.-P. Rocroi, Classification and nomenclator of gastropod families. *Malacologia* **147**, 1–397 (2005).
90. J. B. Knight, Bellerophon muscle scars. *J. Paleontol.* **21**, 264–267 (1947).
91. A. Goriely, "Knotted umbilical cords" in *Physical and Numerical Models in Knot Theory Including Their Application to the Life Sciences*, J. A. Calvo, A. Stasiak, E. Rawdon, Eds. (World Scientific, Singapore, 2004), pp. 109–126.
92. T. McMillan, A. Goriely, Tendril perversion in intrinsically curved rods. *J. Nonlinear Sci.* **12**, 241–281 (2002).
93. R. E. Goldstein, A. Goriely, G. Huber, C. W. Wolgemuth, Bistable helices. *Phys. Rev. Lett.* **84**, 1631–1634 (2000).
94. C. W. Wolgemuth et al., How to make a spiral bacterium. *Phys. Biol.* **2**, 189–199 (2005).
95. A. Goriely, S. Neukirch, Mechanics of climbing and attachment in twining plants. *Phys. Rev. Lett.* **97**, 184302 (2006).
96. D. E. Moulton, H. Oliveri, A. Goriely, Multiscale integration of environmental stimuli in plant tropism produces complex behaviors. *Proc. Natl. Acad. Sci. U.S.A.* **117**, 32226–32237 (2020).
97. T. Lessinnes, D. E. Moulton, A. Goriely, Morphoelastic rods. Part II: Growing birods. *J. Mech. Phys. Solids* **100**, 147–196 (2017).
98. T. van Manen, S. Janbaz, A. A. Zadpoor, Programming the shape-shifting of flat soft matter. *Mater. Today* **21**, 144–163 (2018).
99. D. E. Moulton, T. Lessinnes, A. Goriely, Morphoelastic rods III: Differential growth and curvature generation in elastic filaments. *J. Mech. Phys. Solids* **142**, 104022 (2020).
100. R. Chirat, A. Goriely, D. E. Moulton, Companion mathematica notebook for "The physical basis of mollusk shells chiral coiling – A twisted history." Oxford University Research Archive. <https://ora.ox.ac.uk/objects/uuid:b4d88332-c07b-4294-994d-df3b30b490e9>. Deposited 28 July 2021.